Ecotoxicology and Environmental Safety 252 (2023) 114627

Contents lists available at ScienceDirect

Ecotoxicology and Environmental Safety

journal homepage: www.elsevier.com/locate/ecoenv

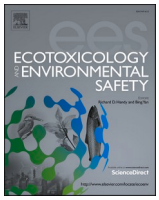

Health risk assessment of heavy metals in road dust from the fourth-tier industrial city in central China based on Monte Carlo simulation and bioaccessibility

Qiao Han [a,b,c], Mingya Wang [c], Xiaohang Xu [a,d], Mengfei Li [e], Yang Liu [c], Chunhui Zhang [c], Shehong Li [a,*], Mingshi Wang [c,*]

[a] State Key Laboratory of Environmental Geochemistry, Institute of Geochemistry, Chinese Academy of Sciences, 550081 Guiyang, China
[b] University of Chinese Academy of Sciences, Beijing 100049, China
[c] College of Resource and Environment, Henan Polytechnic University, 454003 Jiaozuo, China
[d] Key Laboratory of Karst Georesources and Environment, Ministry of Education, Colleage of Resources and Environmental Engineering, Guizhou University, Guiyang 550025, China
[e] Anyang Iron and Steel Group Co. LTD, 455000 Anyang, China

ARTICLE INFO

Edited by Dr. Hao Zhu

Keywords:
Heavy metals
Fourth-tier cities
Exposure risks
Physiologically-based extraction test (PBET)
Source apportionment

ABSTRACT

Health risks caused by heavy metal (HM) exposure in road dust has attracted extensive attention, but few studies have focused on the health risks of residents living in small- and medium-sized cities with rapid industrialization and urbanization. Thus, 140 road dust samples were collected across Anyang, a typical fourth-tier industrial city in central China, which were analysed for 10 different HMs (Mn, Zn, Pb, V, Cr, As, Cd, Ni, Cu and Co). Monte Carlo simulation and bioaccessibility were used to quantify the health risks of heavy metals comprehensively in road dust. Results revealed a remarkable accumulation of Mn, Zn, Pb, Cd and Cu. According to the Geo-accumulation index and potential ecological risk index, Cd was priority control pollutant. Moreover, 55.0% of the road dust samples reached heavily polluted level, and 52.86% of the samples were at high ecological risk levels. These results illustrated that HM contamination was serious and universal in the road dust of Anyang. The occurrences of HMs were allocated to traffic emissions, natural sources, industrial activities and agricultural activities with contribution rates of 35.4%, 6.0%, 41.6% and 17.0%, respectively. Except for Zn in the gastric phase, all other HMs had relatively low bioaccessibilities in the gastrointestinal system, usually less than 20%. The bioaccessibilities of most HMs were higher in the gastric phase, except for Cr, Ni and Cu, which remained higher in the intestinal phase. The non-carcinogenic risk and carcinogenic risk were remarkably reduced when considering the HM bioaccessibilities in the gastrointestinal system, especially for adults. The outcomes of this paper are valuable for understanding HM contamination in road dust and highlight the importance of risk assessment for populations living in the fourth- and fifth-tier cities.

1. Introduction

With the high-intensity development of industrialization and urbanization, heavy metal (HM) contamination in urban environments has been dramatically aggravated worldwide (Jan et al., 2010; Fujiwara et al., 2011; Liu et al., 2016; Pan et al., 2017; Masto et al., 2017; Yadav et al., 2019; Zhao et al., 2022). Owing to the composition and characteristics of road dust, it is regarded as one of the most important carriers of HM contaminants in urban areas (Jayarathne et al., 2018; Chang et al., 2021). In particular, road dust is characterized by a smaller size and a larger specific surface area compared with soils (Gunawardana et al., 2014; Zhao et al., 2016), so HMs in road dust can easily be re-suspended and enter the human body through ingestion, inhalation and dermal contact, potentially threatening the health of urban dwellers (Zhang et al., 2019a; Zgobicki et al., 2019). Thus, conducting detailed investigations on the health risks of HM contamination in road dust is necessary.

In the last few decades, investigations concerning the contamination and health risks of HMs in road dust were numerous and mainly performed in large cities (Shabbaj et al., 2018; Men et al., 2020) and

* Corresponding authors.
E-mail addresses: lishehong@vip.gyig.ac.cn (S. Li), mingshiwang@hpu.edu.cn (M. Wang).

https://doi.org/10.1016/j.ecoenv.2023.114627
Received 23 August 2022; Received in revised form 1 February 2023; Accepted 6 February 2023
Available online 13 February 2023

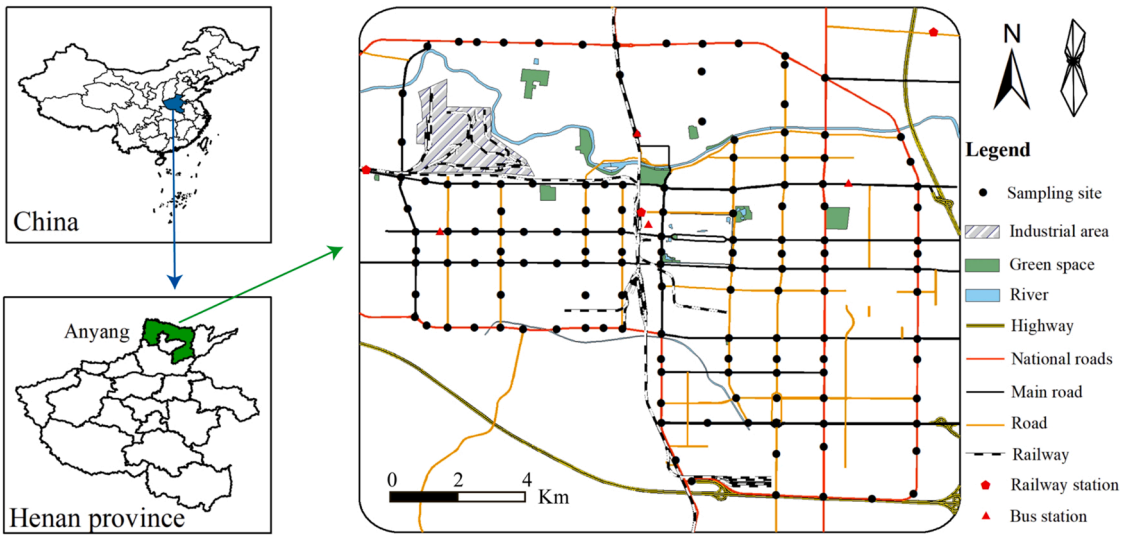

Fig. 1. Study region and sampling locations in Anyang, China.

contaminated areas close to mining areas, industrial parks and thermal power plants (Tian et al., 2019; Khademi et al., 2019; Ahamad et al., 2021). However, these studies ignored the health risks of residents living in rapidly industrializing and urbanization urban areas of small and medium size. In these cities, economic growth was mainly driven by increasing energy consumption and industrial activity, and this is especially true for the fourth- and fifth-tier cities in central China (Zhang et al., 2019b). Fourth- and fifth-tier cities are those with permanent urban residents of less than one million (SCPRC, 2014), and China now has 593 such cities. These small- and medium-sized cities have a higher burden of environmental pollution than large cities because of the extensive production system and underfunded environmental protection (Wang et al., 2022). Only 10% of cities in China have achieved a win–win situation, defined as a relative balance between environmental conservation and economic growth (Wang et al., 2015; Liu et al., 2022). Data concerning the conditions of road dust contaminated by HMs in fourth- and fifth-tier cities are limited. Hence, monitoring the contamination levels of road dust in fourth- and fifth-tier cities, and quantifying the health exposure risk posed by HMs are an urgently needed.

Remarkably, HMs originating from different pollution sources present substantial differences in concentration, toxicity coefficient, bioaccessibility and health risk (Bell et al., 2014; Hou et al., 2017). Identifying the sources of HMs is a prerequisite for preventing new HM inputs and reducing their health risk to humans (Han et al., 2022; Zhao et al., 2022). Many previous studies have proven that compared with principal component analysis, correlation analysis and cluster analysis, the positive matrix factorization (PMF) model can effectively identify and quantify the sources of HMs without constructing the component spectrum of pollution sources (Huang et al., 2021; Sun et al., 2022; Wang et al., 2022). In this paper, geostatistical analysis, correlation analysis and the PMF model were integrated to improve the accuracy of the source apportionment.

Most of the existing studies on health risk assessment largely rely on the total concentrations of HMs by using the Human health risk assessment model with deterministic exposure parameters recommended by the United States Environmental Protection Agency (Gu and Gao, 2018; Zhang et al., 2019a; Jin et al., 2019). However, the uncertainty of HM concentrations and the variability of exposure parameters across different populations and individuals, such as exposure frequency and body weight, may provide inaccurate identification of the high-risk elements and underestimate or overestimate the level of risk (Huang et al., 2022; Zhao et al., 2022). By contrast, Monte Carlo simulation (MCS) produces a more reliable risk assessment by measuring the probability of exceeding and not exceeding risk thresholds. It has been widely applied to assess the health risks of HMs (Chen et al., 2019a and 2019b; Huang et al., 2021). The total concentrations-based assessment has generally ignored the fact that only a fraction of HMs entering the human body can be absorbed (Wang et al., 2016; Han et al., 2020). The actual health risk for humans by road dust ingestion ultimately depends on the fraction of HMs that is available to be dissolved and adsorbed in the human gastrointestinal system (Ning et al., 2021). In recent years, several in vitro bioaccessibility models have been developed and often used to predict the bioaccessibilities of HMs, especially the physiologically-based extraction test (PBET) (Sialelli et al., 2010; Hong et al., 2016; Li et al., 2017). Previous studies have shown a good correlation between the results of PBET digestion experiments and those of in vivo animal experiments (Juhasz et al., 2009; Li et al., 2014; Zheng et al., 2022). Nevertheless, most previous studies solely targeted either the bioaccessibility or MCS in the health risk assessment of HMs while only minute research has expanded on integrating these two approaches in road dust. Therefore, bioaccessibility-based, probabilistic health risks are essential to understand accurately the hazards of HMs contamination in road dust to human health.

The present paper investigated the region of Anyang, which is a typical fourth-tier city in central China's Henan Province. This city experienced rapid industrialization and urbanization in recent decades, and steel smelting activities, energy consumption and transportation have led to serious HM contamination in the atmosphere and soil (Yan et al., 2019; Han et al., 2021; Xu et al., 2021). In 2020, more than 10.4 million tons of standard coal was consumed (AMBS, 2020), and crude steel production was approximately 11.2 million tons, ranking 41st worldwide (WSA, 2021). Additionally, as one of the eight ancient capitals of China, Anyang attracts about 50 million tourists every year, which means that traffic emissions further contribute to HM pollution in the study areas. On this basis, the main objectives of this paper were to investigate the concentrations and in vitro bioaccessibilities of 10 different HMs (Mn, Zn, Pb, V, Cr, As, Cd, Ni, Cu and Co) in road dust from the Anyang urban area, evaluate the contamination levels and probabilistic health risks of HMs in road dust for the study region, and quantitatively discriminate each source of HMs. The findings of this paper will provide helpful guidance for risk managers and policy makers to mitigate HM contamination in fourth- and fifth-tier cities worldwide.

2. Materials and methods

2.1. Study area and sampling

Anyang (N 35°12′−36°22′, E 113°37′−114°58′) is situated in the north of Henan Province and the southeast of Taihang Mountain in central China. The research region has a temperate continental monsoon climate. The average annual temperature, precipitation, relative humidity and wind speed of Anyang are 14.2 °C, 558.4 mm, 65% and 2.2 m/s, respectively (Han et al., 2021). This city has a permanent population of 6.3 million people and covers an area of 7343.9 km^2, including the districts of Wengfeng, Longan, Yindu and Beiguan. The industry is the cornerstone of Anyang's economy, and since 1993, it has been involved in heavy industries, including iron and steel smelting, coking and machinery manufacture.

One hundred and forty road dust samples were collected on local general and national roads across the study area from May 7–13, 2020. Before and during the sampling period, rainfall and gale activity did not occur for 10 days. Road dust samples were collected using a handheld portable vacuum cleaner (Dyson V8 Fluffy) from sidewalks of non-motorized lanes and intersections (Fig. S1). Each sample consisted of four subsamples of approximately 100.0 g. During sampling, the sampling point was away from contaminants such as wet roads, oil stains and large pieces of soil to ensure the quality of samples. After each sampling, sampling tools, such as vacuum cleaner nozzle, suck rod, filter basket, dust collector and brush, were cleaned with deionized water and alcohol to avoid cross-contamination. All samples were then air-dried, homogenized at ambient temperature until constant weight and sieved using a 200 mesh nylon sieve (< 75 μm) for further chemical analysis. (Fig. 1).

2.2. In vitro digestion test

The PBET analytical method was performed according to the previously described studies (Ruby et al., 1996; Gu and Gao, 2018) with minute modification to quantify the bioaccessibilities of HMs in road dust. Briefly, in the gastric phase (PBETG), 1.25 g of pepsin, 0.5 g of citric acid, 0.5 g of malic acid, 0.42 mL of lactic acid, 0.5 mL of glacial acetic acid and 8.775 g of NaCl were dissolved in 1.0 L of deionized water, and the pH was adjusted to 1.5 ± 0.2 with HCl. Next, 2.0 g of each sample was added into a 500 mL cone bottle containing 200.0 ± 5.0 mL simulated gastric solution. The bottle was sealed and then shaken at 100 r·min^{-1} for 1 h in the constant-temperature shaking bath maintained at 37 °C (Guning HZQ-A, China). Then, 30 mL of gastric suspension in each bottle was filtered with 0.45 μm of nitrocellulose membrane for subsequent analysis. In the intestinal phase (PBETI), the remaining mixture pH was adjusted to 8.0 ± 0.2 with $NaHCO_3$ solution. Then, 0.4 g of bile salts and 1.2 g of trypsin were added and sealed, and shaken for 4 h in the same condition. Finally, 30 mL of intestinal suspension was filtered with 0.45 μm of nitrocellulose membrane for further analysis. The bioaccessibilities of HMs (BAF, %) in PBETG and PBETI could be calculated as the percentage of the extracted HM concentrations to the total HM concentrations (Ning et al., 2021; Han et al., 2020). The corresponding equation of BAF is shown in the Supplementary Materials.

2.3. Chemical analysis and quality control

For HM analysis, 0.10 g of sample was poured into a Teflon microwave digestion tube and digested with a mixture of HNO_3 (4.0 mL), H_2O_2 (1.5 mL) and HF (1.5 mL). The total concentration and bioaccessibility of HMs were determined using ICP-OES (PE Optima 8000, USA) and ICP-MS (PE NEXION 300, USA), respectively. During the experiment, glassware and other experiment tools were washed with 10% HNO_3 and deionized water (Ulupure UPD-II-40 L, China), and all the chemical reagents were of high purity. Moreover, 20% of reagent blanks, 10% of parallel samples and national standard reference materials (GBW07401) were analysed simultaneously for quality control. Relative standard deviations based on the mean values obtained for each sample were less than 15%.

2.4. Evaluation methods of HMs pollution

Geo-accumulation index (I_{geo}), improved Nemerow index (*INI*) developed by Liu et al. (2020), and potential ecological risk index (*E* and *RI*) were calculated to estimate overall pollution and individual pollution of HMs considered. I_{geo}, *INI*, *E* and *RI* are calculated by Eqs. (1–3) as follows:

$$I_{geo} = \log[C_s/(1.5 \times C_b)], \quad (1)$$

$$INI = \sqrt{(I^2_{geo_{max}} + I^2_{geo_{avg}})/2}, \quad (2)$$

$$RI = \sum E^i_r = \sum T^i_r \quad (3)$$

where C_s is the concentration of HMs in the road dust sample; C_b is the regional background value of these elements; $I_{geo\ max}$ and $I_{geo\ avg}$ are the max and average values of I_{geo}, respectively. *E* is the ecological risk for single elements; T^i_r is the toxic response coefficient. The values of T^i_r for Mn, Zn, Pb, V, Cr, As, Cd, Ni, Cu and Co are 1, 1, 5, 2, 2, 10, 30, 5, 5 and 5, respectively (Hakanson, 1980; Teng et al., 2014). The I_{geo}, *INI*, *E* and *RI* are unitless. The pollution degrees of I_{geo}, *INI*, *E* and *RI* are detailed in Table S1.

2.5. Probabilistic health risk calculation

HM exposure to the human body can occur via paths of oral ingestion, inhalation and dermal contact (Tian et al., 2019). According to the United States Environmental Protection Agency (USEPA, 1989, 2009, 2011), the average daily intake dose (*ADD*, mg/kg·day) can be calculated by Eqs. (4–6):

$$ADD_{ingest} = (c \times R_{ingest} \times EF \times ED \times 10^{-6})/(BW \times AT) \quad (4)$$

$$ADD_{inhal} = (c \times R_{inhal} \times EF \times ED)/(BW \times AT \times PEF) \quad (5)$$

$$ADD_{dermal} = (c \times SA \times SL \times ABS \times EF \times ED \times 10^{-6})/(BW \times AT) \quad (6)$$

Additionally, this method has been revised and supplemented by Environmental Planning Specialists given that HMs entering the human body are not completely soluble and absorbed (EPS, 2011). Thus, the risk assessment model needs to be modified based on the gastrointestinal bioaccessibilities of HMs, as shown in Eqs. (7–8):

$$ADD_{inhal} - PBETG = (c \times R_{inhal} \times EF \times ED \times BAF_G)/(BW \times AT \times PEF), \quad (7)$$

$$ADD_{inhal} - PBETI = (c \times R_{inhal} \times EF \times ED \times BAF_I)/(BW \times AT \times PEF), \quad (8)$$

where BAF_G and BAF_I are the bioaccessibilities of HMs in PBETG and PBETI, respectively. The carcinogenic risk (*CRs*) and non-carcinogenic risks (*NCRs*) can be calculated by Eqs. (9–10):

$$HI = \sum HQ = \sum ADD/RfD, \quad (9)$$

$$TCR = \sum CR = \sum ADD \times SF, \quad (10)$$

where hazard index (*HI*) and total carcinogenic risk (*TCR*) are the summation of the potential risk of all individual hazard quotient (*HQ*) and carcinogenic (*CR*), respectively (Han et al., 2020). For *CNRs*, an *HQ* or *HI* > 1 indicates a potential adverse health risk, conversely *NCRs* (USEPA, 2011). For *CRs*, if the *CR* or *TCR* exceeds 1.0E-04, humans

Table 1
Concentrations (mg/kg) of HMs in road dust of Anyang and other cities around the world.

Elements	Mn	Zn	Pb	V	Cr	As	Cd	Co	Ni	Cu
Minimum	274.8	43.0	17.3	25.7	23.1	7.7	0.3	2.2	6.7	6.4
Maximum	6022.8	1599.4	400.2	312.4	253.7	37.7	8.9	15.8	47.4	267.2
Mean	1244.1	332.0	88.7	86.8	97.6	18.4	2.4	7.4	19.0	53.2
Median	938.9	264.8	72.4	73.6	88.9	17.6	2.1	7.0	17.8	41.3
Standard deviation	907.5	233.5	62.4	44.0	37.8	4.7	1.3	2.1	7.1	41.2
Kurtosis	2.9	2.6	2.5	2.2	1.1	1.2	1.8	1.3	1.6	2.3
Skewness	11.0	9.0	8.9	5.8	1.9	2.4	5.3	3.0	3.5	7.0
Coefficient of variance/%	72.9	70.3	70.4	50.6	38.8	25.3	55.6	28.6	37.4	77.4
Background value[a]	554.0	58.4	25.4	90.1	62.5	10.9	0.1	9.7	30.0	19.2
Guide values[b]	n/a	n/a	400.0	165.0	30.0	20.0	20.0	20.0	150.0	2000.0
Shijiazhuang, China[c]	540.0	238.8	42.1	n/a	59.8	15.5	n/a	36.5	24.5	44.0
Xi'an, China[d]	510.5	268.6	124.5	69.6	145	n/a	n/a	30.9	30.8	54.7
Zhengzhou, China[e]	117.3	192.2	27.0	n/a	45.3	22.5	2.7	n/a	n/a	39.8
Tianjing, China[f]	670.6	983.2	120.7	100.2	n/a	29.5	2.1	10.5	77.9	527.5
Jinan, China[g]	517.0	492.8	80.3	51.8	114.1	n/a	1.1	8.2	30.3	87.7
Moscow,Russia[h]	641.0	1026.0	91.0	81.0	68.0	2.0	0.8	15.0	46.0	184.0
Tehran, Iran[i]	864.0	666.0	213.0	n/a	76.5	5.4	0.8	n/a	57.7	275.0
Uttar Pradesh, India[j]	417.0	98.2	23.6	n/a	39.64	6.9	0.2	n/a	22.2	34.0
Jeddah, Saudi Arabia[k]	550.6	487.5	140.7	80.9	65.4	21.6	7.5	11.7	51.3	139.1

[a] CNEMC (1990); [b] MEE (2018); [c] Zuo et al. (2022); [d] Pan et al. (2017); [e] Zhu et al. (2021); [f] Zhang et al. (2019a); [g] Dong et al. (2020); [h] Vlasov et al. (2021); [i] Dehghani et al. (2017); [j] Ahamad et al. (2021); [k] Shabbaj et al. (2018).

suffer from substantial risks of cancer; if the *CR* or *TCR* ranges from 1.0E-6–1.0E-4, the *CR* is acceptable; if the *CR* or *TCR* is below 1E-06, the *CR* is negligible (USEPA, 1989). Other parameters, including their meaning and values in the exposure risk models, are described in Tables S2 and S3. At the same time, MCS was used to reduce the deviation of results generated by using HM concentration outliers and fixed parameters, and the random simulation times were 100,000 times (Chen et al., 2019b).

2.6. PMF model

PMF model has been widely applied to discriminate quantitatively the contribution of sources to samples (Huang et al., 2021; Zhao et al., 2022). This model first decomposed the concentration matrix into factor contribution matrix and factor profile matrix, and then based on the characteristics of each pollution source, determined the contribution rate of each factor (Paatero and Tapper, 1994; Lian et al., 2019). PMF model can be calculated by Eq. (11):

$$X_{ij} = \sum_{k=1}^{p} g_{ik} f_{kj} + e_{ij}, \tag{11}$$

where x_{ij} is the concentration of HMs (the *i*th sample of *j*th chemical species); p is the number of sources; g_{ik} denotes the contribution of the source to the sample; f_{kj} indicates the amount of HMs from source; e_{ij} represents the residual matrix. According to Eqs. (12–14), the optimal solution of PMF model is obtained by minimizing the sum of the 'objective function' Q (Guan et al., 2019; Salim et al., 2019).

$$Q = \sum_{i=1}^{n} \sum_{j=1}^{m} \left(\frac{e_{ij}}{u_{ij}}\right)^2, \tag{12}$$

$$\text{For} x_{ij} \le MDL, u_{ij} = \frac{5}{6} \times MDL, \tag{13}$$

$$\text{For} x_{ij} > \text{MDL}, u_{ij} = \sqrt{(\sigma \times x_{ij})^2 + (0.5 \times \text{MDL})^2}, \tag{14}$$

where u_{ij} refers to the uncertainty of HMs, *MDL* is the method detection limit of HMs and σ is the error fraction of HMs.

2.7. Data analysis

Statistical analysis involved Microsoft Office 2019, SPSS 23.0 (IBM, USA) and Origin 2021 (©Origin Lab Corporation, USA) software. Spatial distributions of *INI*, *RI*, HM concentrations and bioaccessibilities were performed through Inverse Distance Weighted interpolation using ArcGIS 10.2 (ESRI, CA, USA). MCS was adopted for uncertainty analyses using Crystal Ball (©Oracle, CA, USA) software.

3. Results and discussion

3.1. HM concentrations in road dust

Descriptive characteristics of HMs in road dust of Anyang are presented in Table 1. The mean concentrations of Mn, Zn, Pb, V, Cr, As, Cd, Ni, Cu and Co were 1244.1, 332.0, 88.7, 86.8, 97.6, 18.4, 2.4, 19.0, 53.2 and 7.4 mg/kg, respectively. Except for V, Co and Ni, all other HM concentrations were greater than the regional background values of Henan Province, China (CNEMC, 1990). Especially, the concentrations of Zn, Pb and Cd were 5.69, 3.49 and 34.29 times higher than their relevant arithmetic average background values, respectively (Fig. S2a). Additionally, Mn, Zn, Pb, As, Cd and Cu in more than 90% of the samples were higher than the background values, indicating that these HMs have been widely enriched. Compared with the national guide values, the maximum concentrations of Pb, V, Cr and As exceeded the corresponding soil environmental quality standard (MEE, 2018). According to the coefficients of variation (CVs) (Han et al., 2020), Mn, Zn, Pb, V, Cr, Cd, Ni and Cu exhibited substantial spatial variation (CV > 35%), notably Mn, Zn, Pb and Cu with CVs of 72.9%, 70.3%, 70.4% and 77.4%, respectively. This finding indicated that HMs in road dust of Anyang had considerable spatial variability, implying the substantial influence from nearby anthropogenic activities (Hou et al., 2019). Moreover, the skewness values of Mn, Zn, Pb, V, Cd and Cu were remarkably higher than those of other elements, and their maximum concentrations were 6022.8, 1599.4, 400.2, 312.4, 8.9 and 267.2 mg/kg, respectively, which were considerably higher than the soil background values (Table 1). This result reflected that some points might be highly affected by human emissions (Jin et al., 2019; Huang et al., 2021).

Table 1 lists the comparison of the average concentrations of HMs in road dust from Anyang with those of other investigated cities around the world. Compared with other cities, the average concentrations of Zn, Pb, As, and Cu in Anyang's road dust samples were intermediate level. The average concentration of Mn from Anyang was higher than that in the other cities, but the average concentration of Co and Ni was lower. The mean concentration of Cd from Anyang was only lower than that in the commercial capital of Saudi Arabia (Jeddah) (Shabbaj et al., 2018) and

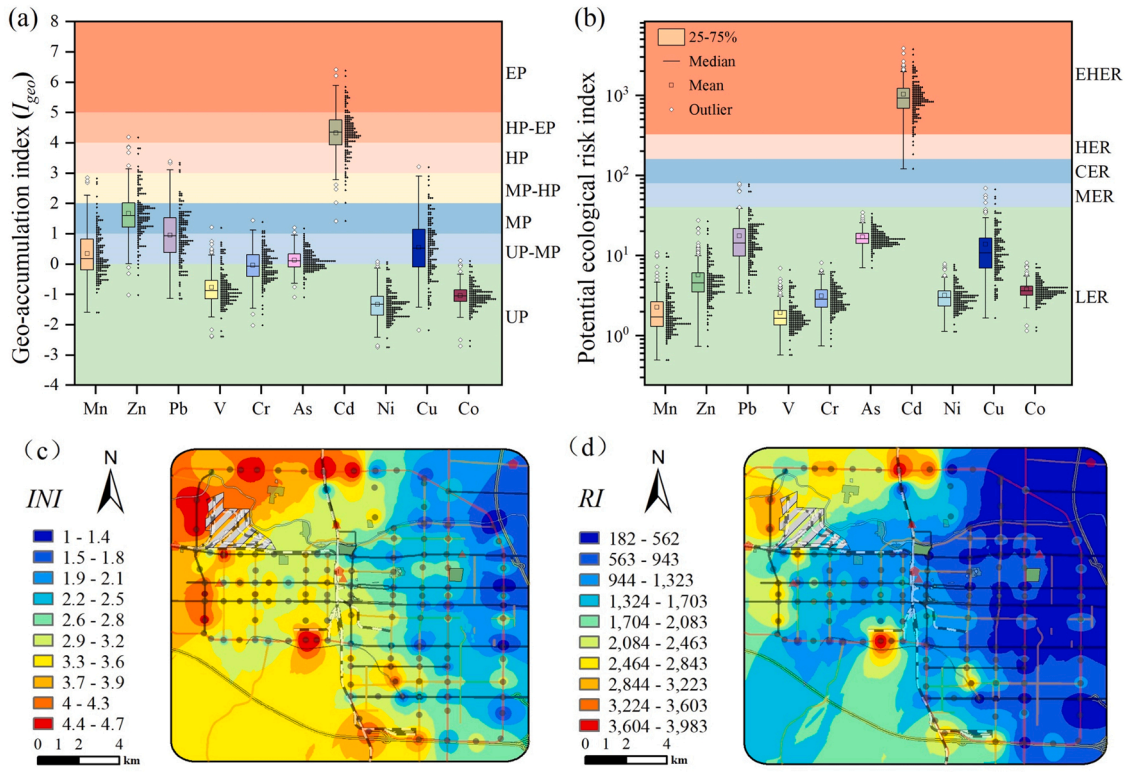

Fig. 2. Contamination assessment of HMs in road dust of Anyang.

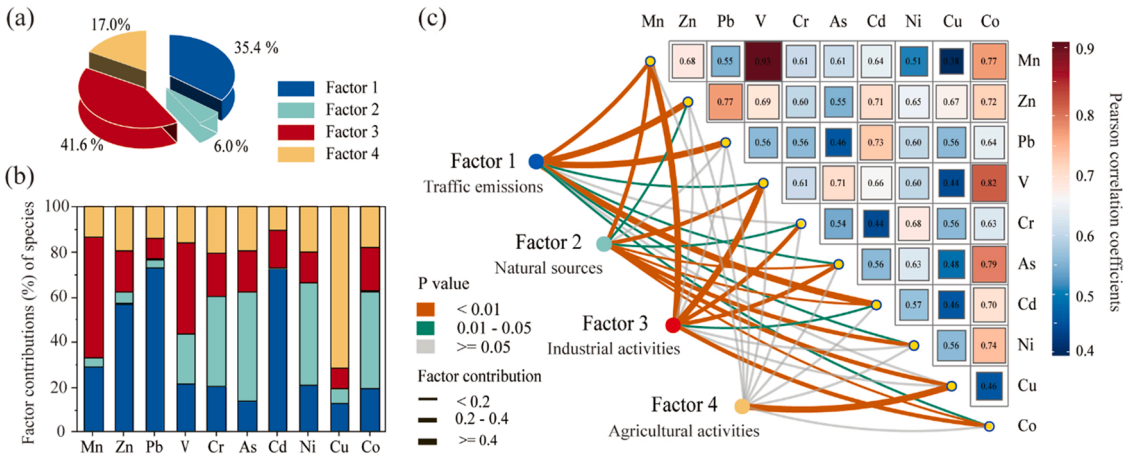

Fig. 3. (a) Source apportionment of HMs in road dust from Anyang. (b) (a): Percentage contributions of factors for total HMs, (b): Source profiles of factors for each HMs, (c): Correlation coefficients of HMs concentrations and four factors.

central China (Zhengzhou), an important transportation hub between north and south China (Zhu et al., 2021), and the mean concentrations of V and Cr were all lower than that in the metropolis in central China (Xi'an) (Pan et al., 2017). All these suggested that besides traffic-related emissions, industrial production, commerce or certain other factors substantially influence HMs in road dust such as Cd and Mn (Hou et al., 2019).

3.2. Contamination assessment of HMs in road dust

The contamination levels and values for I_{geo}, *INI*, *E* and *RI* of HMs in road dust of Anyang are shown in Fig. 2 and Tables S4 and S5. The basic trend of mean I_{geo} values of HMs was Cd > Zn > Pb > Cu > Mn > As > Cr > V> Co > Ni. Generally, Cd with the highest mean I_{geo} value of 4.32 showed moderately to heavily polluted (MP-HP), followed by Zn (1.67) classified as moderately polluted (MP). Lead (0.95), Cu (0.54), Mn (0.34) and As (0.13) had the mean I_{geo} values at the level of unpolluted to moderately polluted (UP-MP). The mean I_{geo} values of Cr, Co and Ni were < 1, indicating unpolluted (UP). In all samples, 5.7%, 2.9%, 21.4% and 0.7%, the I_{geo} values of Zn, Pb, Cd and Cu, respectively, were more than 3.0 (Table S6), signifying heavily polluted (HP). The basic trend of mean *E* values of HMs was in the range of Cd > Pb > As > Cu > Zn > Co > Ni > Cr > Mn > V, demonstrating that except for Cd (extremely high ecological risk, EHER), all the other elements were classified as low ecological risk (LER), as shown in Fig. 3b and Table S4. Additionally, Mn, Zn, Cr, Ni and Co in all samples and 97.1% of Pb and Cu samples with *E* values < 40 showed LER. For Cd, 95.7% of the *E* value were > 320, representing EHER.

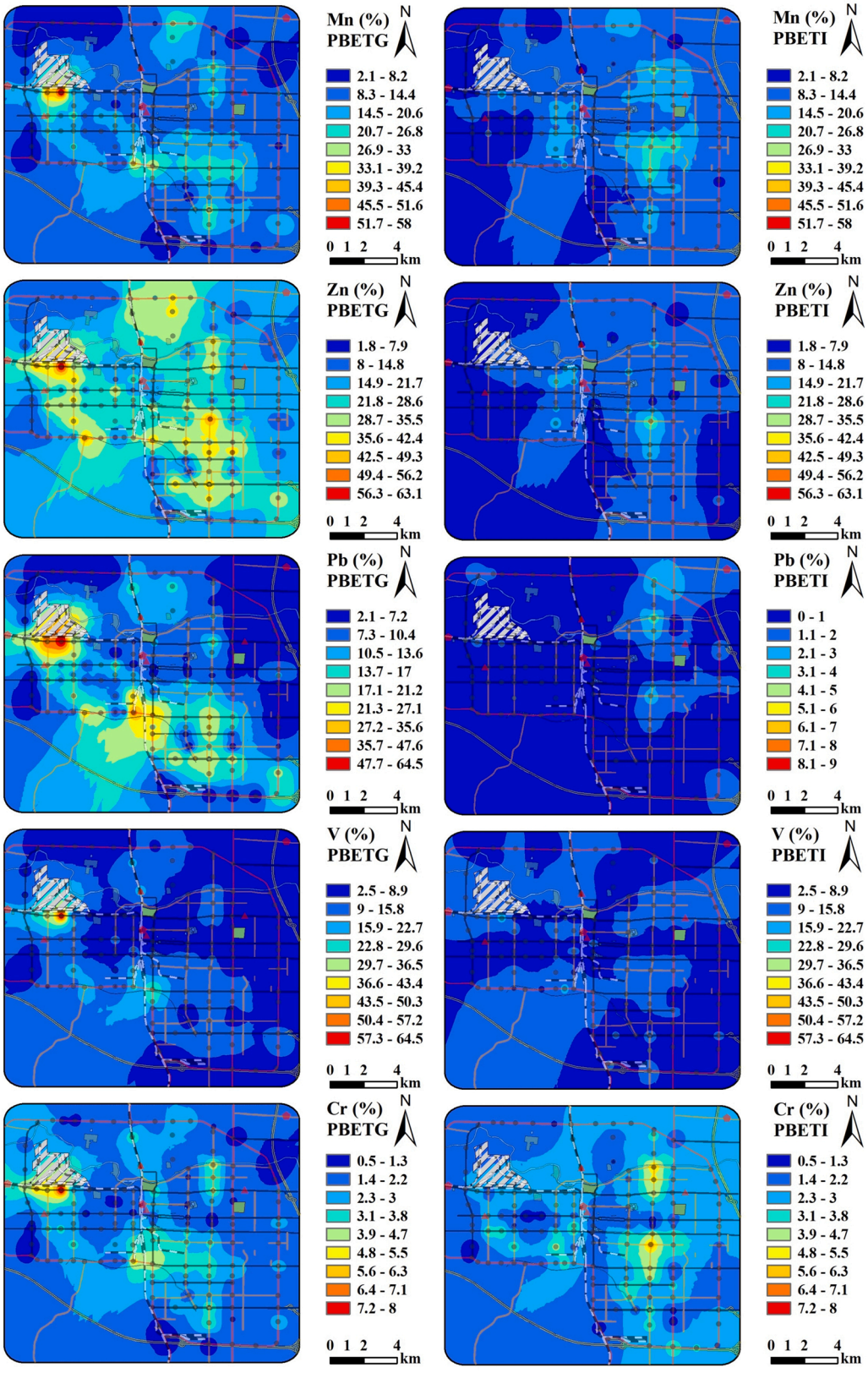

Fig. 4. Spatial distributions of gastrointestinal bioaccessibilities of HMs in road dust of Anyang, China.

The mean *INI* values of HMs followed the order Cd > Zn > Pb > Cu > Mn > Cr > V > Ni > As > Co, and the *INI* value for all samples varied from 1.01 to 4.66 with a mean of 3.09, demonstrating the stratified spatial heterogeneity of HM pollution degree in the survey area (**Fig. S2b**). Amongst all samples, 34.3% of *INI* values were categorized into MP-HP, whereas 55.0% of them were at HP level with the remaining

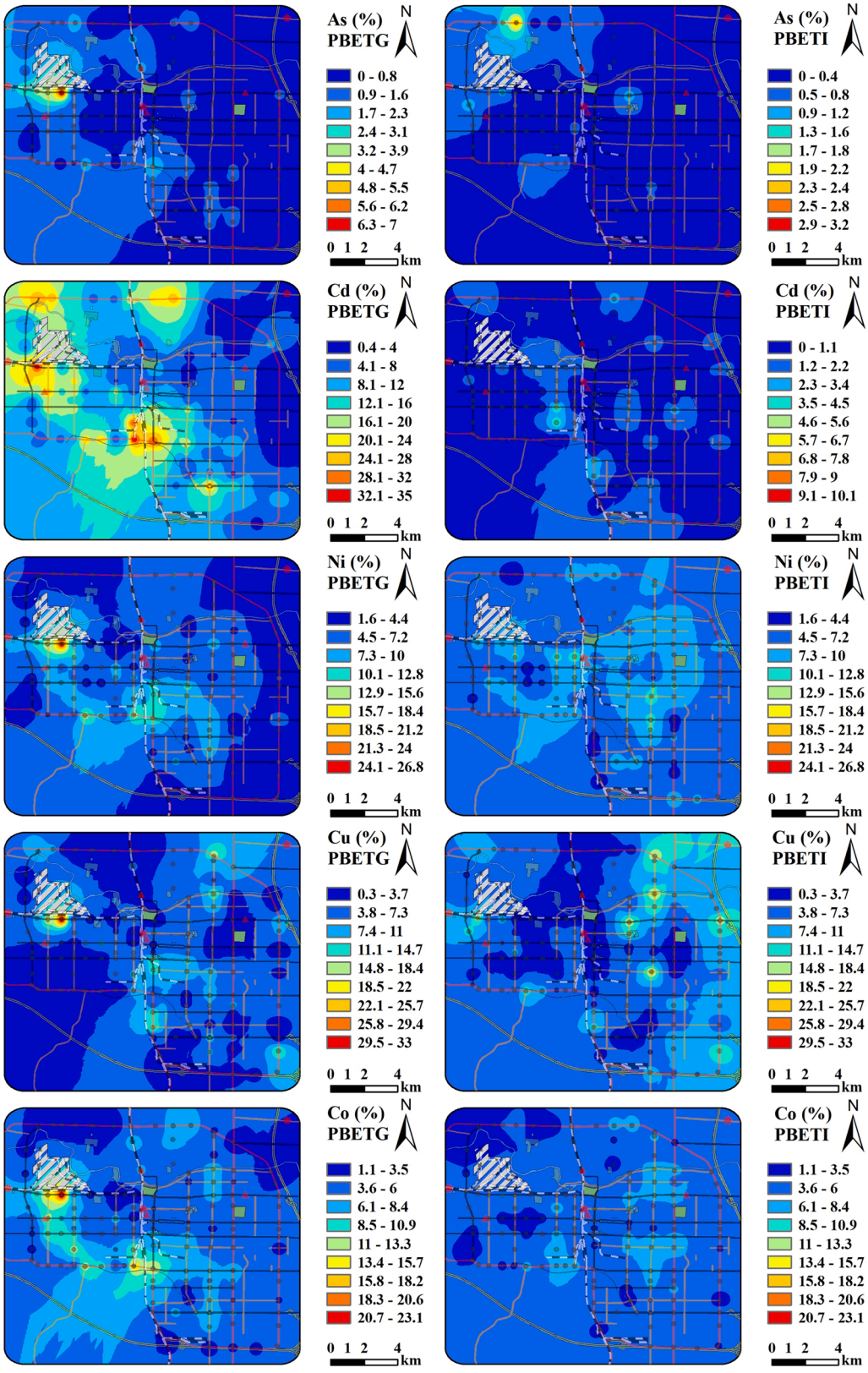

Fig. 4. (*continued*).

7.1% of the total samples at heavy to extremely polluted (HP-EP) level (**Table S5**). The *RI* values of HMs determined in road dust ranged from 172.6 to 3988.2 with a mean of 1094.8 (**Table S4**), and Cd accounted for a substantial portion of *RI* due to the high mean *E* of Cd. The combined ecological risk of the HMs presented a moderate risk (MER) level in 2.1% samples, considerable potential risk (CER) level in 15.0% samples, high potential risk (HER) level in 52.9% samples and EHER level in 30.0% samples. The overall pollution degree of HMs in road dust from Anyang

Table 2
Bioaccessiblities of HMs in the gastric and intestinal phase of road dust in Anyang, China.

HMs	Concentration (mg/kg)		Gastric (%)		Intestinal (%)		Residual (%)	
	Range	Mean	Range	Mean	Range	Mean	Range	Mean
Mn	274.81–6022.80	1244.14	2.51–58.48	13.94	2.10–28.59	11.58	24.98–95.40	74.48
Zn	43.00–1599.40	332.04	4.74–62.62	23.63	1.75–32.07	9.05	14.22–91.98	67.32
Pb	17.28–400.22	88.66	2.09–64.71	11.46	0.00–3.89	0.69	34.12–97.26	87.85
V	25.7–312.4	86.8	2.79–64.68	10.17	2.56–20.01	8.82	15.73–94.14	81.01
Cr	23.06–253.73	97.64	0.51–7.98	2.21	0.52–6.13	2.40	89.41–98.96	95.40
As	7.65–37.67	18.44	0.01–6.90	0.79	0.00–2.27	0.27	92.16–99.96	98.94
Cd	0.28–8.94	2.40	0.37–34.49	10.62	0.00–5.21	0.91	62.98–99.31	88.47
Ni	6.72–47.42	19.00	1.60–25.66	5.74	2.34–13.37	6.82	64.51–94.89	87.44
Cu	6.35–267.15	53.23	0.30–33.11	4.86	0.26–19.67	5.92	58.54–98.88	89.22
Co	2.22–15.80	7.36	1.12–23.43	5.47	1.71–8.90	4.70	70.30– 96.94	89.84

was universal and severe. Furthermore, the *INI* and *RI* with high values were mostly found in the northwest and southwest of the study area, and low values were mainly distributed in the central, northeast and southeast of the study area (Figs. 2**c and** 2**d**). These high-value areas of *INI* and *RI* were mainly found around industrial areas (e.g. smelters, machinery processing plants and thermal power plants) and intersections, suggesting that anthropogenic activities may be the dominant sources of HM contamination in road dust.

3.3. Source apportionment of HMs in road dust

To discriminate quantitatively the contribution rate of pollution sources to HMs, this paper correlated the Pearson correlation analysis with the factor contributions from PMF model (Fig. 3**a–c**). Collinearity analysis was performed firstly on the original data, and all HMs with variance inflation factor > 10 and tolerance > 0.1 were revealed to be suitable for further analysis (Peng et al., 2021). In PMF model, a minimum and stable objective function Q value was obtained when the number of factors was four (Chen et al., 2019b). Almost all of the residuals were within − 3–3, and the minimum fitting coefficients (r^2) of HMs between the observed and predicted concentrations were greater than 0.50 (**Table S6**), indicating an accurate, rational result. Consequently, four factors were extracted, and their contribution percentages for total HMs in Anyang road dust were 35.4%, 6.0%, 41.6% and 17.0%, respectively (Fig. 3**a**). Moreover, geographical statistical analysis was applied to identify accurately the source apportionment (Zhao et al., 2022). The spatial distributions of HM concentrations were showed in **Fig. S3**.

Factor 1, with a contribution rate of 35.4% (Fig. 3**a**), can be interpreted as traffic emissions. This factor was mainly characterized by Zn (56.7%), Pb (72.7%) and Cd (72.3%) (**Table S6**). Relatively high correlations (r > 0.70) were found between these HMs, suggesting common sources (Jin et al., 2019). Moreover, the GIS map showed that these elements with high concentrations were mainly distributed along national roads in the study area (**Fig. S3**). Generally, vehicular exhaust, braking and tire wear are responsible for Cd, Pb and Zn contamination (Mielke et al., 2011). Although the nationwide prohibition of leaded petrol was taken on July 1, 2000, in China, a considerable concentration of Pb still exists in the urban environment because of its half-life of hundreds of years (Wang et al., 2020). Moreover, Pb has been used historically in lead-based paint production because Pb can improve the adhesion of paint to substrate/surfaces (Gilbert and Weiss, 2006), enhance colours (O'Connor et al., 2018) or strengthen crack resistance (Crow, 2007). $PbCO_3$ and $PbCrO_4$ are widely applied in the white and yellow traffic line markings, respectively. Therefore, this factor was considered the consequence of traffic emissions.

Factor 2, accounting for 6.0% of the total variance (Fig. 3**a**), may have been associated with natural sources. This factor mainly loaded on Cr (40.1%), As (48.5%), Ni (45.4%) and Co (43.1%) (**Table S6**). Cobalt and Ni could be attributed to the natural background because their mean concentrations in the road dust of Anyang were below the regional background values (Table 1). Moreover, Cr, As and Ni and Co had relatively lower CV values than the other HMs (Table 1). 53.6%, 37.9%, 98.6% and 99.3% the I_{geo} value of Cr, As, Co and Ni were lower than 0, indicating unpolluted (**Table S5**). Arsenic and Cr have also been confirmed to originate feasibly from soil parent materials/geogenic sources (Facchinelli et al., 2001; Egodawatta et al., 2013). Hence, Factor 2 was allocated to natural sources, with minute influence from anthropogenic sources.

Factor 3, which accounted for 41.6% of the total variance (Fig. 3**a**), might be assigned to industrial activities. This factor had high loading values for Mn (53.6%) and V (40.3%), and low loadings for Co (19.4%), Cr (19.0%), Zn (18.6%), As (18.3%) and Cd (16.7%), as shown in **Table S6**. Vanadium, a strategically important metal, is widely used in the steel industry. Estimates showed that ferrovanadium in the steel industry accounts for approximately 85% of the produced global vanadium (Yang et al., 2017; Li et al., 2020). By 2020, more than 200 small- and medium-scale ferroalloy enterprises, and a large-scale steel smelter (Anyang Steel Plant) existed in Anyang (AMBS, 2020). Although China's environmental regulators have adopted strict emission limits, abundant quantities of V have been released into the environment as a result of metal smelting, machine manufacturing and coal consumption (Jin et al., 2019). A remarkable association (0.93) was found between V and Mn (Fig. 3**c**), and the GIS map confirmed that the hotspots of Mn and V were concentrated in the western part of the research region (**Fig. S3**), indicating a potential common source. Moreover, previous studies found that Mn enrichment was pronounced in surface soil and atmosphere surrounding iron and steel smelters (Kelepertzis et al., 2020; Soltani et al., 2021). Thus, Factor 3 was identified as industrial activities.

Factor 4, accounting for 17.0% of the total variance (Fig. 3**a**), may have been associated with agricultural activities. This factor was weighted heavily on Cu (71.8%) and less than 25% of other HMs (**Table S6**). Many flower plants were planted along and in the middle of the urban road. To protect them from noxious bacteria and pests, bactericides and pesticides containing Cu or As are widely used, which would be deposited directly or indirectly into road dust (Zhang et al., 2018). Moreover, the GIS map showed that the concentration of Cu showed a relatively uniform spatial distribution (**Fig. S3**). Therefore, Factor 4 was principally derived from agricultural activities, such as bactericides and pesticide dissemination.

3.4. Bioaccessibilities of HMs in road dust

Percent gastrointestinal bioaccessibilities of HMs in road dust of Anyang based on PBET are plotted in Fig. 4 and Table 2. The average PBETG bioaccessibilities of HMs followed the order Zn > Mn > Pb > Cd > V > Ni > Co > Cu > Cr > As, and PBETI bioaccessibilities followed the order Mn > Zn > V > Ni > Cu > Co > Cr > Cd > Pb > As. Amongst all HMs, Zn, Mn and V had relatively high bioaccessibilities in the gastrointestinal system, which was consistent with previous research (Gu and Gao, 2018; Han et al., 2020). In PBETG and PBETI, Zn, Mn and V were mostly present in the acid-soluble and extractable forms, and

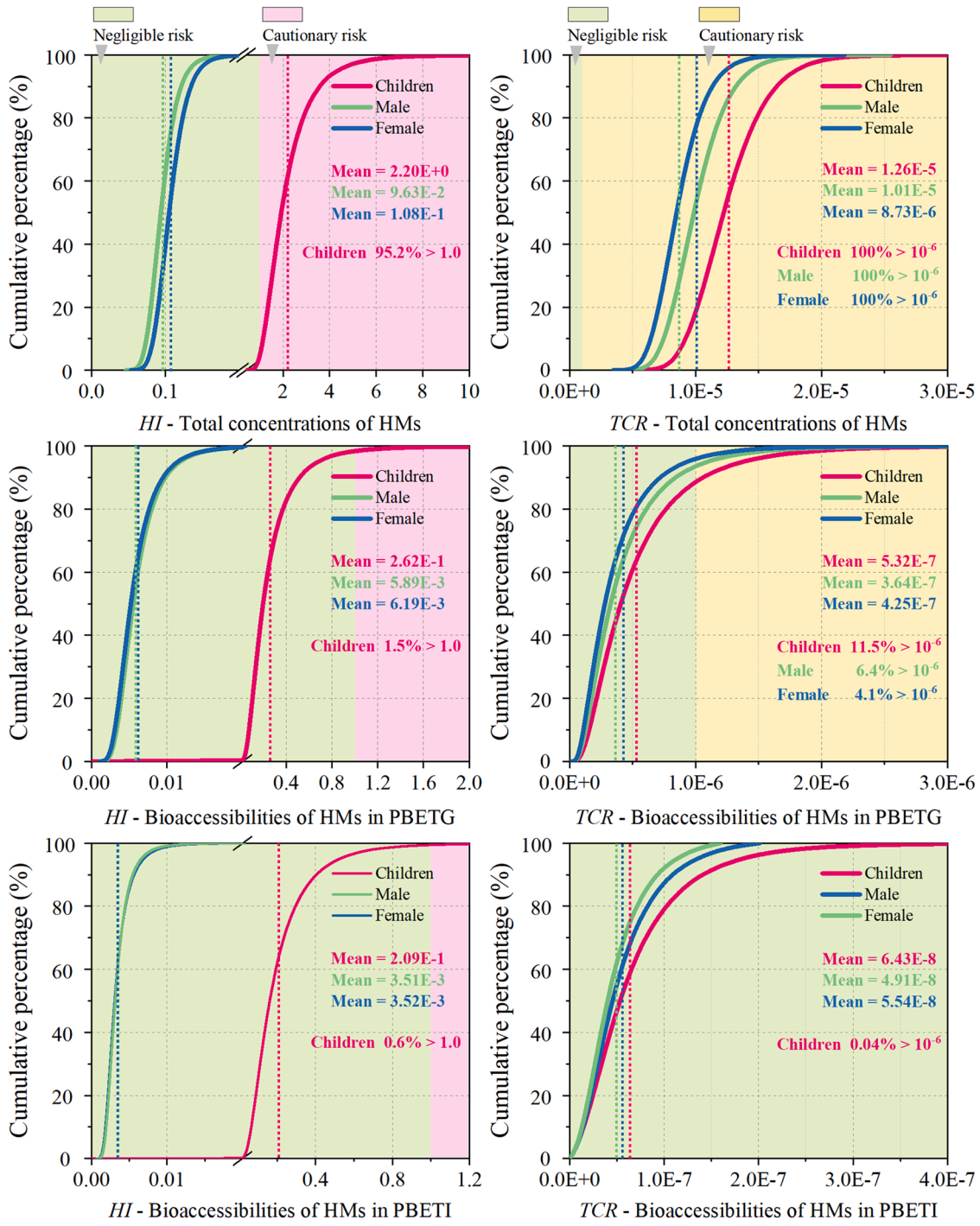

Fig. 5. Health risk (*HI* and *TCR*) of HMs in road dust based on total concentrations and bioaccessibilities of HMs in PBETG and PEBTI.

easily digested and dissolved by human gastrointestinal fluid (Wragg et al., 2011; Zheng et al., 2020). Arsenic demonstrated the lowest bioaccessibility in the two phases, which might be related to their large residual phase and the chemical composition of iron in the samples (He et al., 2020). The iron-rich matter with a large specific surface area was conducive to the adsorption or precipitation of As (V) and As (III), which led to the low bioaccessibility (Pan et al., 2014; Khanam et al., 2019).

The bioaccessibilities of Mn, Zn, Pb, V, As, Cd and Co in PBETG were higher than that in PBETI, and their bioaccessibilities in PBETI decreased by 17.0%, 61.7%, 94.0%, 13.2%, 65.8%, 91.5% and 14.1%, respectively. In PBETG, the pH value was 1.5, which was substantially lower than that in PBETI. In this case, the activity of digestive enzymes increased, and HMs were easily dissolved (Mingot et al., 2011; Zhang et al., 2019a). However, after entering PBETI, the pH value changed from acidic (1.5) to alkaline (8.0). HMs were prone to adsorption and precipitation reactions, so these elements in the intestinal solution would be passivated and fixed again (Pelfrene et al., 2011). The bioaccessibilities of Cr, Ni and Cu in PBETG were more than those in the corresponding PBETI. Amongst them, Cu was prone to chemical complexation reaction with bile salts and trypsin in the intestinal fluid under neutral conditions, and exhibited high water solubility (Zheng et al., 2013; Ai et al., 2018). In addition, the GIS map showed that samples with the higher bioaccessibilities of Mn, Zn, Pb, Cr, Cd, Ni, Cu and Co in PBETG and PBETI were mainly distributed in the centre of the

study area, whereas V and As with higher PBETG and PBETI bioaccessibilities were observed in the west and northwest of the study area (Fig. 4). Relatively substantial differences in the spatial distributing characteristics of HMs between gastric and intestinal bioaccessibilities and concentrations were found (Table 1 **and 2**), which indicated that HM concentrations were not the dominant factors to influence their bioaccessibilities. Previous studies indicated that bioaccessibility might be associated with the condition of the study region (industrial structure, traffic intensity and functional areas), sample characteristics (particle size, conductivity, pH and organic matter content) and metal speciation (Patinha et al., 2015; Wu et al., 2015). Therefore, health risk assessment based on HM bioaccessibilities would be closer to the actual risk for humans than that based on HMs concentrations.

3.5. Probabilistic health risk assessment

The HM bioaccessibilities and MCS were adopted to evaluate the probabilistic *NCRs* and *CRs* of residents' exposure to HMs in road dust from Anyang. For adult females and males, the average values of *HI* based on total concentrations of HMs were 1.08E-1 and 9.63E-2, respectively, indicating negligible *NCRs* (Fig. 5). However, the mean value of *HI* for children was 2.20E+ 0 (range: 4.20E-1 – 2.23E+1), which was more than two times greater than the USEPA's recommended value of 1.0 (**Table S7**). Nearly 95% of *HI* value with a 95% confidential range of 1.01E+ 0–4.33E+ 0 was greater than 1 for children, indicating high *NCRs* (**Table S7**). Manganese and As were proven to be the dominant factors in *NCRs* for children and adults, respectively, by comparing the *HQ* value of HMs (**Table S7**). Especially, the *HQ* value of Mn for children was greater than 1.0 even in the 70th percentile. Although Cd had high I_{geo} and *E*, its *NCRs* was below 1.0 due to the low ratio of intake dose to body weight (**Tables S5 and S7**). However, because the total HMs in road dust cannot be absorbed completely in the gastrointestinal system, the above probabilistic *NCRs* would be overestimated (Denys et al., 2012; Zheng et al., 2020). After incorporating the bioaccessibilities of HMs by PBETG and PBETI, the mean values of *HQ* and *HI* were substantially reduced (Fig. 5). Especially, the mean value of *HI* for adult females and males sharply decreased (PBETG: 6.19E-3, 5.89E-3; PBETI: 3.52E-3, 3.51E-3), implying that the probability of *NCRs* could not occur.

Based on the total concentrations of HMs studied, the average values of *TCR* for children, adult females and males were 1.26E-5, 1.01E-5 and 8.73E-6, respectively, which indicated that the *CRs* were cautionary in the study region (Fig. 5). Meanwhile, 100.0% of *TCR* value for all populations surpassed 1E-06, which indicated that residents might be exposed to considerable potential *CRs* (Fig. 5). According to **Table S7**, the basic order of average *CR* value of HMs for all groups was as As > Cd > Cr > Pb > Co > Ni. The average *CR* values of these elements for all populations varied from 1.0E-10–1.0E-4, indicating that *CRs* were under the acceptable level. Similarly, after incorporating the bioaccessibilities of HMs by PBETG and PBETI, the average values of *CR* and *TCR* decreased dramatically (Fig. 5). Only the *TCR* value for children in the range between 1.0E-06 and 1.0E-04 were approximately 10% (PBETG) and 5% (PBETI), respectively (**Table S7**), indicating the probabilistic *CRs*. According to the above results, the *NCRs* and *CRs* based on bioaccessibilities of HMs can lower health risks to residents, which was consistent with previous research (Zheng et al., 2020; Ning et al., 2021). However, the probability that *NCRs* and *CRs* may occur in this study area, especially for children, remains high.

4. Conclusion

The present paper revealed the contamination characteristics, source apportionments, bioaccessibilities and probabilistic health risks of HMs in road dust from a typical fourth-tier cities in central China. The results revealed that Mn, Zn, Pb, As, Cd and Cu in Anyang road dust were elevated owing to the influence of different anthropogenic activities. Especially, Zn, Pb, and Cd were 5.69, 3.49 and 34.29 times greater than the background values of Henan Province, China, respectively. Cadmium with the highest average I_{geo} and *E* exhibited MP-HP and EHER. PMF model combined with the geostatistical analysis identified four sources dominating HM contamination in road dust (traffic emissions, natural sources, industrial activities and agricultural activities), accounting for 35.4%, 6.0%, 41.6% and 17.0% of the total HM contents, respectively. The percent gastrointestinal bioaccessibilities of HMs (except Zn in PBETG) was lower than 20%, and exhibited marked variance between PBETG and PBETI. Amongst them, Mn, Zn, Pb, V, As, Cd and Co had relatively greater bioaccessibilities in PBETG than in PBEGI, but the opposite was observed for Cr, Ni and Cu. The *HI* value for local children was higher than the USEPA's recommended value of 1.0 even at the 5th percentile, implying high potential *NCRs*. Therefore, greater focus should be placed on the children. Overall, these findings provided comprehensive knowledge for understanding the contamination and corresponding health risk of HMs from the fourth or fifth-tier cities.

CRediT authorship contribution statement

Qiao Han: Data analysis, Writing – original draft, Writing – review & editing, Validation. **Mingya Wang**, **Xiaohang Xu**: Writing – review & editing, Visualization. **Mengfei Li:** Investigation, Sampling, Experimental execution. **Chunhui Zhang:** Methodology, Software, Visualization. **Shehong Li** and **Mingshi Wang:** Conceptualization, Project administration, Supervision.

Declaration of Competing Interest

The authors declare that they have no known competing financial interests or personal relationships that could have appeared to influence the work reported in this paper.

Data Availability

Data will be made available on request.

Acknowledgments

This work was supported by the Strategic Priority Research Program of the Chinese Academy of Sciences (XDB40020405) and National Natural Science Foundation of China (42177070).

Appendix A. Supporting information

Supplementary data associated with this article can be found in the online version at doi:10.1016/j.ecoenv.2023.114627.

References

Ahamad, A., Raju, N.J., Madhav, S., Gossel, W., Ram, P., Wycisk, P., 2021. Potentially toxic elements in soil and road dust around Sonbhadra industrial region, Uttar Pradesh, India: source apportionment and health risk assessment. Environ. Res. 11685.

Ai, Y.W., Li, X.P., Gao, Y., Zhang, M., Zhang, Y.C., Zhang, X., Yan, X.Y., Liu, B., Yu, H.T., 2018. In vitro bioaccessibility of potentially toxic metals (PTMs) in Baoji urban soil (NW China) from different functional areas and its implication for health risk assessment. Environ. Geochem. Health 41, 1055–1073.

AMBS (Anyang City Municipal Bureau of Statistics), 2020. Anyang City Statistical Yearbook in 2020. China Statistics Press, Beijing.

Bell, M.L., Ebisu, K., Leaderer, B.P., Gent, J.F., Lee, H.J., Koutrakis, P., Wang, Y., Dominici, F., Peng, R.D., 2014. Associations of PM2.5 constituents and sources with hospital admissions: analysis of four counties in Connecticut and Massachusetts (USA) for Persons >= 65 years of age. Environ. Health Perspect. 122, 138–144.

Chang, X., Yu, Y., Li, Y.X., 2021. Response of antimony distribution in street dust to urban road traffic conditions. J. Environ. Manag. 296, 113219.

Chen, B., Wang, X.B., Li, Y.L., Yang, Q., Li, J.S., 2019a. Energy-induced mercury emissions in global supply chain networks: structural characteristics and policy implications. Sci. Total Environ. 670, 87–97.

Chen, R.H., Chen, H.Y., Song, L.T., Yao, Z.P., Meng, F.S., Teng, Y.G., 2019b. Characterization and source apportionment of heavy metals in the sediments of Lake Tai (China) and its surrounding soils. Sci. Total Environ. 694, 133819.
CNEMC (China National Environmental Monitoring Centre), 1990. The Soil Background Value in China. China Environmental Science Press, Beijing.
Crow, J.M., 2007. Why Use Lead in Paint?.
Dehghani, S., Moore, F., Keshavarzi, B., Hale, B.A., 2017. Health risk implications of potentially toxic metals in street dust and surface soil of Tehran, Iran. Ecotoxicol. Environ. Saf. 136, 92–103.
Denys, S., Caboche, J., Tack, K., Rychen, G., Wragg, J., Cave, M., Jondreville, C., Feidt, C., 2012. In vivo validation of the unified BARGE method to assess the bioaccessibility of arsenic, antimony, cadmium, and lead in soils. Environ. Sci. Technol. 46 (11), 6252–6260.
Dong, S.Z., Zhang, S.W., Wang, L.J., Ma, G., Lu, X.W., Li, X.P., 2020. Concentrations, speciation, and bioaccessibility of heavy metals in street dust as well as relationships with physiochemcal properties: a case study of Jinan city in East China. Environ. Sci. Pollut. Res. 27 (28), 35724–35737.
Egodawatta, P., Ziyath, A.M., Goonetilleke, A., 2013. Characterising metal build-up on urban road surfaces. Environ. Pollut. 176, 87–91.
EPS (Environmental Planning Specialists), 2011. Revised Draft Human Health Baseline Risk Assessment for Upland Soils. Kirk Kessler, Principal.
Facchinelli, A., Sacchi, E., Mallen, L., 2001. Multivariate statistical and GIS-based approach to identify heavy metal sources in soils. Environ. Pollut. 114, 313–324.
Fujiwara, F., Rebagliati, R.J., Dawidowski, L., Gómez, D., Polla, G., Pereyra, V., Smichowski, P., 2011. Spatial and chemical patterns of size fractionated road dust collected in a megacitiy. Atmos. Environ. 45, 1497–1505.
Gilbert, S.G., Weiss, B., 2006. A rationale for lowering the blood lead action level from 10 to 2 μg/dL. Neurotoxicology 27, 693–701.
Gu, Y., Gao, Y., 2018. Bioaccessibilities and health implications of heavy metals in exposed-lawn soils from 28 urban parks in the megacity Guangzhou inferred from an in vitro physiologically-based extraction test. Ecotoxicol. Environ. Saf. 148, 747–753.
Guan, Q., Zhao, R., Pan, N., Wang, F., Yang, Y., Luo, H., 2019. Source apportionment of heavy metals in farmland soil of Wuwei, China: comparison of three receptor models. J. Clean. Prod. 237, 117792.
Gunawardana, C., Egodawatta, P., Goonetilleke, A., 2014. Role of particle size and composition in metal adsorption by solids deposited on urban road surfaces. Environ. Pollut. 184, 44–53.
Hakanson, L., 1980. An ecological risk index for aquatic pollution control: a sediment ecological approach. Water Res. 14, 975–1001.
Han, J.L., Liang, L.C., Zhu, Y.R., Xu, X.H., Wang, L., Shang, L.H., WU, P., WU, Q.X., Qian, X.L., Qiu, G.L., Feng, X.B., 2022. Heavy metal(loid)s in farmland soils on the Karst Plateau, Southwest China: an integrated analysis of geochemical baselines, source apportionment, and associated health risk. Land. Degrad. Dev. 33, 1689–1703.
Han, Q., Wang, M.S., Cao, J.L., Gui, C.L., Liu, Y.P., He, X.D., He, Y.C., Liu, Y., 2020. Health risk assessment and bioaccessibilities of heavy metals for children in soil and dust from urban parks and schools of Jiaozuo, China. Ecotoxicol. Environ. Saf. 191, 110157.
Han, Q., Liu, Y., Feng, X.X., Mao, P., Sun, A., Wang, M.Y., Wang, M.S., 2021. Pollution effect assessment of industrial activities on potentially toxic metal distribution in windowsill dust and surface soil in Central China. Sci. Total Environ. 759, 144023.
He, A., Li, X.P., Ai, Y.W., Li, X.L., Zhang, Y.C., Gao, Y., Liu, B., Zhang, X., Zhang, M., Peng, L.Y., Zhou, M., Yu, H.T., 2020. Potentially toxic metals and the risk to children's health in a coal mining city: an investigation of soil and dust levels, bioaccessibility and blood lead levels. Environ. Int. 141, 105788.
Hong, J., Wang, Y.D., McDermott, S., Cai, B., Aelion, C.M., Lead, J., 2016. The use of a physiologically-based extraction test to assess relationships between bioaccessible metals in urban soil and neurodevelopmental conditions in children. Environ. Pollut. 212, 9–17.
Hou, D.Y., O'Connor, D., Nathanail, P., Tian, L., 2017. Integrated GIS and multivariate statistical analysis for regional scale assessment of heavy metal soil contamination: a critical review. Environ. Pollut. 231, 1188–1200.
Hou, S.G., Zheng, N., Tang, L., Ji, X.F., Li, Y.Y., Hua, X.Y., 2019. Pollution characteristics, sources, and health risk assessment of human exposure to Cu, Zn, Cd and Pb pollution in urban street dust across China between 2009 and 2018. Environ. Int. 128, 430–437.
Huang, J.L., Wu, Y.Y., Sun, J.X., Li, X., Geng, X.L., Zhao, M.L., Sun, T., Fan, Z.Q., 2021. Health risk assessment of heavy metal(loid)s in park soils of the largest megacity in China by using Monte Carlo simulation coupled with Positive matrix factorization model. J. Hazard. Mater. 415, 125629.
Huang, S.Y., Li, Q., Liu, H., Ma, S.T., Long, C.Y., Li, G.Y., Yu, Y.X., 2022. Urinary monohydroxylated polycyclic aromatic hydrocarbons in the general population from 26 provincial capital cities in China: levels, influencing factors, and health risks. Environ. Int. 160, 107074.
Jan, F.A., Ishaq, M., Ihsanullah, I., S, M., Asim, S.M., 2010. Multivariate statistical analysis of heavy metals pollution in industrial area and its comparison with relatively less polluted area: a case study from the City of Peshawar and district Dir lower. J. Hazard. Mater. 176, 609–616.
Jayarathne, A., Egodawatta, P., Ayoko, G.A., Goonetilleke, A., 2018. Intrinsic and extrinsic factors which influence metal adsorption to road dust. Sci. Total Environ. 618, 236–242.
Jin, Yl, David, O., Yong, S.O., Daniel, C.W.T., An, L., Hou, D.Y., 2019. Assessment of sources of heavy metals in soil and dust at children's playgrounds in Beijing using GIS and multivariate statistical analysis. Environ. Int. 124, 320–328.
Juhasz, A.L., Weber, J., Smith, E., Naidu, R., Rees, M., Rofe, A., Kuchel, T., Sansom, L., 2009. Assessment of four commonly employed in vitro arsenic bioaccessibility assays for predicting in vivo relative arsenic bioavailability in contaminated soils. Environ. Sci. Technol. 43, 9487–9494.
Kelepertzis, E., Argyraki, A., Chrastn, V., Botsou, F., Fouskas, A., Skordas, K., Komarek, M., Fouskas, A., 2020. Metal(loid) and isotopic tracing of pb in soils, road and house dusts from the industrial area of Volos (central Greece). Sci. Total Environ. 725, 138300.
Khademi, H., Gabarrón, M., Abbaspour, A., Martínez-Martínez, S., Faz, A., Acosta, J.A., 2019. Environmental impact assessment of industrial activities on heavy metals distribution in street dust and soil. Chemosphere 217, 695–705.
Khanam, R., Kumar, A., Nayak, A.K., Shahid, M., Pathak, H., 2019. Metal(loid)s (As, Hg, Se, Pb and Cd) in paddy soil: bioaccessibility and potential risk to human health. Sci. Total Environ. 699, 134330.
Li, H.B., Li, J., Juhasz, A.L., Ma, L.Q., 2014. Correlation of in vivo relative bioavailability to in vitro bioaccessibility for arsenic in household dust from China and its implication for human exposure assessment. Environ. Sci. Technol. 48, 13652–13659.
Li, H.H., Chen, L.J., Yu, L., Guo, Z.B., Shan, C.Q., Lin, J.Q., Gu, Y.G., Yang, Z.B., Yang, Y. X., Shao, J.R., Zhu, X.M., Cheng, Z., 2017. Pollution characteristics and risk assessment of human exposure to oral bioaccessibility of heavy metals via urban street dust from different functional areas in Chengdu, China. Sci. Total Environ. 586, 1076–1084.
Li, Y.N., Zhang, B.G., Liu, Z.Q., Wang, S., Yao, J., Borthwick, A.G.L., 2020. Vanadium contamination and associated health risk of farmland soil near smelters throughout China. Environ. Pollut. 263, 114540.
Lian, C., Zhou, S.L., Wu, S.H., Wang, C.H., He, D., 2019. Concentration, fluxes, risks, and sources of heavy metals in atmospheric deposition in the Lihe River watershed, Taihu region, eastern China. Environ. Pollut. 255 (2), 113301–113301.
Liu, L., Liu, A., Li, Y., Zhang, L.X., Zhang, G.J., Guan, Y.T., 2016. Polycyclic aromatic hydrocarbons associated with road deposited solid and their ecological risk: implications for road stormwater reuse. Sci. Total Environ. 563–564, 190–198.
Liu, L.L., Liu, Q.Y., Ma, J., Wu, H.W., Qu, Y.J., Gong, Y.W., Yang, S.H., An, Y.F., Zhou, Y. Z., 2020. Heavy metal(loid)s in the topsoil of urban parks in Beijing, China: concentrations, potential sources, and risk assessment. Environ. Pollut. 260, 114083.
Liu, X.H., Liu, Y., Wang, B.H., 2022. Evaluating the sustainability of Chinese cities: indicators based on a new data envelopment analysis model. Ecol. Indic. 137, 108779.
Masto, R., George, J., Rout, T., Ram, L., 2017. Multi element exposure risk from soil and dust in a coal industrial area. J. Geochem. Explor. 176, 100–107.
MEE (Ministry of Ecology and Environment), 2018. GB 36600–2018, Soil Quality Standard: Risk Control Standard for Soil Contamination of Development Land. Ministry of Ecology and Environment.
Men, C., Liu, R.M., Xu, L.B., Wang, Q.R., Guo, L.J., Miao, Y.X., Shen, Z.Y., 2020. Source-specific ecological risk analysis and critical source identification of heavy metals in road dust in Beijing, China. J. Hazard. Mater. 388, 121763.
Mielke, H.W., Laidlaw, M.A., Gonzales, C.R., 2011. Estimation of leaded (Pb) gasoline's continuing material and health impacts on 90 US urbanized areas. Environ. Int. 37, 248–257.
Mingot, J., Miguel, E.D., Chacón, Enrique, 2011. Assessment of oral bioaccessibility of arsenic in playground soil in madrid (Spain): a three-method comparison and implications for risk assessment. Chemosphere 84 (10), 1386–1391.
Ning, Z.P., Liu, E.G., Yao, D.J., Xiao, T.F., Ma, L., Liu, Y.Z., Li, H., Liu, C.S., 2021. Contamination, oral bioaccessibility and human health risk assessment of thallium and other metal(loid)s in farmland soils around a historic Tl\\Hg mining area. Sci. Total Environ. 758, 143577.
O'Connor, D., Hou, D.Y., Ye, J., Zhang, Y.H., Ok, Y.S., Song, Y.N., Coulon, F., Peng, T.Y., Tian, L., 2018. Lead-based paint remains a major public health concern: a critical review of global production, trade, use, exposure, health risk, and implications. Environ. Int. 121, 85–101.
Paatero, P., Tapper, U., 1994. Positive matrix factorization: a non-negative factor model with optimal utilization of error estimates of data values. Environmetrics 5 (2), 111–126.
Pan, H.Y., Lu, X.W., Lei, K., 2017. A comprehensive analysis of heavy metals in urban road dust of Xi'an, China: contamination, source apportionment and spatial distribution. Sci. Total Environ. 609, 1361–1369.
Pan, W., Wu, C.N., Xue, S.G., Hartley, W., 2014. Arsenic dynamics in the rhizosphere and its sequestration on rice roots as affected by root oxidation. J. Environ. Sci. 26 (4), 892–899.
Patinha, C., Reis, A.P., Dias, A.C., Abduljelil, A.A., Noack, Y., Robert, S., Cave, M., Silva, E.F.D., 2015. The mobility and human oral bioaccessibility of Zn and Pb in urban dusts of Estarreja (N Portugal). Environ. Geochem. Health 37 (1), 115–131.
Pelfrene, A., Waterlot, C., Mazzuca, M., Nisse, C., Bidar, G., Douay, F., 2011. Assessing Cd, Pb, Zn human bioaccessibility in smelter-contaminated agricultural topsoils (Northern France). Environ. Geochem. Health 33 (5), 477–493.
Peng, X., Zhang, L., Li, Y., Lin, Q.W., He, C., Huang, S.Z., Li, H., Zhang, X.Y., Liu, B.Y., Ge, F.J., Zhou, Q.H., Zhang, Y., Wu, Z.B., 2021. The changing characteristics of phytoplankton community and biomass in subtropical shallow lakes: Coupling effects of land use patterns and lake morphology. Water Res. 200 (15), 117235.
Ruby, M.V., Davis, A., Schoof, R., Eberle, S., Sellstone, C.M., 1996. Estimation of lead and arsenic bioaccessibility using a physiologically based extraction test. Environ. Sci. Technol. 30 (2), 422–430.
Salim, I., Sajjad, R.U., Paule–Mercado, M.C., Memon, S.A., Lee, B.-Y., Sukhbaatar, C., Lee, C.-H., 2019. Comparison of two receptor models PCA–MLR and PMF for source identification and apportionment of pollution carried by runoff from catchment and

sub–watershed areas with mixed land cover in South Korea. Sci. Total Environ. 663, 764–775.
SCPRC (The State Council of the People's Republic of China), 2014. Notice of The State Council on Adjusting the Standards for Dividing the size of Cities. http://www.gov.cn/zhengce/content/2014–11/20/content_9225.htm.
Shabbaj, I.I., Alghamdi, M.A., Shamy, M., Hassan, S.K., Alsharif, M.M., Khoder, M.I., 2018. Risk assessment and implication of human exposure to road dust heavy metals in Jeddah, Saudi Arabia. Int. J. Environ. Res. Public Health 15 (1), 36.
Sialelli, J., Urquhart, G.J., Davidson, C.M., Hursthouse, A.S., 2010. Use of a physiologically based extraction test to estimate the human bioaccessibility of potentially toxic elements in urban soils from the city of glasgow, UK. Environ. Geochem. Health 32 (6), 517–527.
Soltani, N., Keshavarzi, B., Moore, F., Cave, M., Sorooshian, A., Mahmoudi, M.R., Ahmadi, M.R., Golshani, R., 2021. In vitro bioaccessibility, phase partitioning, and health risk of potentially toxic elements in dust of an iron mining and industrial complex. Ecotoxicol. Environ. Saf. 212, 111972.
Sun, J.X., Zhao, M.L., Huang, J.L., Liu, Y.F., Wu, Y.Y., Cai, B.Y., Han, Z.W., Huang, H.H., Fan, Z.Q., 2022. Determination of priority control factors for the management of soil trace metal(loid)s based on source-oriented health risk assessment. J. Hazard. Mater. 432, 127116.
Teng, Y.G., Wu, J., Lu, S.J., Wang, Y.Y., Jiao, X.D., Song, L.T., 2014. Soil and soil environmental quality monitoring in China: a review. Environ. Int. 69, 177–199.
Tian, S.H., Tao, L., Li, K.X., 2019. Road dust contamination in a mining area presents a likely air pollution hotspot and threat to human health. Environ. Int. 128, 201–209.
USEPA (United States Environmental Protection Agency), 1989. Risk Assessment Guidance for Superfund Volume I: Human Health Evaluation Manual (Part A). U.S. Environment Protection Agency (Washington DC).
USEPA (United States Environmental Protection Agency), 2009. Risk Assessment Guidance for Superfund (RAGS). U.S. Environment Protection Agency (Washington DC).
USEPA (United States Environmental Protection Agency), 2011. Exposure Factors Handbook, Final ed. U.S. Environment Protection Agency (Washington DC).
Vlasov, D., Kosheleva, N., Kasimov, N., 2021. Spatial distribution and sources of potentially toxic elements in road dust and its PM_{10} fraction of Moscow megacity. Sci. Total Environ. 761 (3), 143267.
Wang, F.F., Guan, Q.Y., Tian, J., Lin, J.K., Yang, Y.Y., Yang, L.Q., Pan, N.H., 2020. Contamination characteristics, source apportionment, and health risk assessment of heavy metals in agricultural soil in the hexi corridor. Catena 191, 104573.
Wang, J.H., Li, S.W., Cui, X.Y., Li, S.W., Cui, X.C., Li, H.M., Qian, X., Wang, C., Sun, Y.X., 2016. Bioaccessibility, sources and health risk assessment of trace metals in urban park dust in Nanjing, southeast China. Ecotoxicol. Environ. Saf. 128, 161–170.
Wang, Q.W., Zhao, Z.Y., Shen, N., Liu, T.T., 2015. Have Chinese cities achieved the win-win between environmental protection and economic development? From the perspective of environmental efficiency. Ecol. Indic. 51, 151–158.
Wang, W.J., Chen, C., Liu, D., Wang, M.S., Han, Q., Zhang, X.C., Feng, X.X., Sun, A., Mao, P., Xiong, Q.Q., Zhang, C.H., 2022. Health risk assessment of $PM_{2.5}$ heavy metals in county units of northern China based on Monte Carlo simulation and APCS-MLR. Sci. Total Environ. 843, 156777.
Wragg, J., Cave, M., Basta, N., Brandon, E., Casteel, S., Denys, S., Gron, C., Oomen, A., Reimer, K., Tack, K., Wiele, T.V.D., 2011. An inter-laboratory trial of the unified BARGE bioaccessibility method for arsenic, cadmium and lead in soil. Sci. Total Environ. 409 (19), 4016–4030.
WSA (World Steel Association), 2021. List of companies with tonnage of more than 3 million tonnes (Mt) in 2020.
Wu, Q., Leung, J.Y.S., Geng, X., Chen, S., Huang, X., Li, H., 2015. Heavy metal contamination of soil and water in the vicinity of an abandoned e-waste recycling site: implications for dissemination of heavy metals. Sci. Total Environ. 506–507, 217–225.
Xu, X.T., Han, Q., Wang, M.Y., Shen, J., Guo, X.M., Wang, M.Y., 2021. Pollution characteristics and health risk assessment of heavy metals in soil of large industrial areas and surrounding communities in Anyang city. Earth Environ. 49 (5), 551–560.
Yadav, I.C., Devi, N.L., Singh, V.K., Li, J., Zhang, G., 2019. Spatial distribution, source analysis, and health risk assessment of heavy metals contamination in house dust and surface soil from four major cities of Nepal. Chemosphere 218, 1100–1113.
Yan, L., Du, X.S., He, J.Y., Wang, K., Wang, L.J., Zhang, R.Q., 2019. Emission characteristics of particulate matter and carbon components from coal-fired sources in Anyang. Ecol. Environ. Sci. 28 (8), 1604–1612.
Yang, J., Teng, Y.G., Wu, J., Chen, H.Y., Wang, G.Q., Song, L.T., Yue, W.F., Zuo, R., Zhai, Y.Z., 2017. Current status and associated human health risk of vanadium in soil in China. Chemosphere 171, 635–643.
Zgobicki, W., Telecka, M., Skupinski, S., 2019. Assessment of short-term changes in street dust pollution with heavy metals in Lublin (*E* Poland)-levels, sources and risks. Environ. Sci. Pollut. Res. 26, 35049–35060.
Zhang, H., Mao, Z., Huang, K., Wang, X., Cheng, L., Zeng, L., Zhou, Y., Jing, T., 2019a. Multiple exposure pathways and health risk assessment of heavy metal (loid) s for children living in fourth-tier cities in Hubei Province. Environ. Int. 129, 517–524.
Zhang, J., Wu, L., Zhang, Y., Li, F., Fang, X., Mao, H., 2019b. Elemental composition and risk assessment of heavy metals in the PM_{10} fractions of road dust and roadside soil. Particuology 44 (3), 7.
Zhang, P., Qin, C., Hong, X., Kang, G., Qin, M., Yang, D., Pang, B., Li, Y., He, J., Dick, R. P., 2018. Risk assessment and source analysis of soil heavy metal pollution from lower reaches of Yellow River irrigation in China. Sci. Total Environ. 633, 1136–1147.
Zhao, N., Lu, X., Chao, S., 2016. Risk assessment of potentially toxic elements in smaller than 100μm street dust particles from a valley–city in northwestern China. Environ. Geochem. Health 38 (2), 483–496.
Zhao, Z.J., Hao, M., Li, Y.L., Li, S.H., 2022. Contamination, sources and health risks of toxic elements in soils of karstic urban parks based on Monte Carlo simulation combined with a receptor model. Sci. Total Environ. 839, 156223.
Zheng, N., Hou, S.N., Wang, S.J., Sun, S.Y., An, Q.R., Li, P.Y., Li, X.Q., 2020. Health risk assessment of heavy metals in street dust around a zinc smelting plant in China based on bioaccessibility and bioaccessibility. Ecotoxicol. Environ. Saf. 197, 110617.
Zheng, S.A., Wang, F., Li, X.H., Wang, H., Wan, X.C., 2013. Application of in vitro digestion approach for estimating lead bioaccessibility in contaminated soils: influence of soil properties. Res. Environ. Sci. 26 (8), 851–857.
Zheng, X.M., Zhang, Z.Y., Chen, J.C., Liang, H.T., Chen, X., Qin, Y., Shohag, M.J.I., Wei, Y.Y., Gu, M.H., 2022. Comparative evaluation of in vivo relative bioavailability and in vitro bioaccessibility of arsenic in leafy vegetables and its implication in human exposure assessment. J. Hazard. Mater. 423, 126909.
Zhu, H.N., Liu, X.L., Xu, C.H., Zhang, L.B., Chen, H.Y., Shi, F., Li, Y., Liu, Y.Z., Zhang, B. Z., 2021. The health risk assessment of Heavy Metals (HMs) in road dust based on Monte Carlo simulation and bio-toxicity: a case study in Zhengzhou, China. Environ. Geochem. Health 36, 5135–5156.
Zuo, L., Lu, X.W., Fan, P., Wang, L.Q., Yu, B., Lei, K., Yang, Y.F., Chen, Y.R., 2022. Concentrations, sources and ecological–health risks of potentially toxic elements in finer road dust from a megacity in north China. J. Clean. Prod. 358, 132036.